**Title**

Technical Note: Simulation of 4DCT tumor motion measurement errors

**Permalink**

https://escholarship.org/uc/item/4s34w5th

**Authors**

Dou, Tai H
Thomas, David H
O'Connell, Dylan
et al.

Peer reviewed

# Technical Note: Simulation of 4DCT tumor motion measurement errors

Tai H. Dou,[a)] David H. Thomas, and Dylan O'Connell
*Department of Radiation Oncology, University of California Los Angeles, Los Angeles, California 90095*

Jeffrey D. Bradley
*Department of Radiation Oncology, Washington University of St. Louis School of Medicine, St. Louis, Missouri 63110*

James M. Lamb and Daniel A. Low
*Department of Radiation Oncology, University of California Los Angeles, Los Angeles, California 90095*

**Purpose:** To determine if and by how much the commercial 4DCT protocols under- and overestimate tumor breathing motion.

**Methods:** 1D simulations were conducted that modeled a 16-slice CT scanner and tumors moving proportionally to breathing amplitude. External breathing surrogate traces of at least 5-min duration for 50 patients were used. Breathing trace amplitudes were converted to motion by relating the nominal tumor motion to the 90th percentile breathing amplitude, reflecting motion defined by the more recent 5DCT approach. Based on clinical low-pitch helical CT acquisition, the CT detector moved according to its velocity while the tumor moved according to the breathing trace. When the CT scanner overlapped the tumor, the overlapping slices were identified as having imaged the tumor. This process was repeated starting at successive 0.1 s time bin in the breathing trace until there was insufficient breathing trace to complete the simulation. The tumor size was subtracted from the distance between the most superior and inferior tumor positions to determine the measured tumor motion for that specific simulation. The effect of the scanning parameter variation was evaluated using two commercial 4DCT protocols with different pitch values. Because clinical 4DCT scan sessions would yield a single tumor motion displacement measurement for each patient, errors in the tumor motion measurement were considered systematic. The mean of largest 5% and smallest 5% of the measured motions was selected to identify over- and underdetermined motion amplitudes, respectively. The process was repeated for tumor motions of 1–4 cm in 1 cm increments and for tumor sizes of 1–4 cm in 1 cm increments.

**Results:** In the examined patient cohort, simulation using pitch of 0.06 showed that 30% of the patients exhibited a 5% chance of mean breathing amplitude overestimations of 47%, while 30% showed a 5% chance of mean breathing amplitude underestimations of 36%; with a separate simulation using pitch of 0.1 showing, respectively, 37% overestimation and 61% underestimation.

**Conclusions:** The simulation indicates that commercial low-pitch helical 4DCT processes potentially yield large tumor motion measurement errors, both over- and underestimating the tumor motion. © 2015 American Association of Physicists in Medicine. [http://dx.doi.org/10.1118/1.4931416]

Key words: 4DCT, irregular breathing, amplitude sorting, phase sorting

## 1. INTRODUCTION

4DCT has been proposed to characterize the patient anatomical changes due to breathing motion.[1–3] The integration of 4DCT into treatment planning has the potential of reducing tumor position uncertainties due to respiratory motion so that the treatment condition can be simulated as realistically as possible. Inaccurate estimation of breathing motion by 4DCT, however, can yield systematic errors in motion margins and inappropriate selection of motion mitigation strategies.

The generation of 4DCT images usually involves the simultaneous imaging of the anatomical site and the recording of an external surrogate signal. Analysis of the images or CT projections and the breathing cycle is used to generating CT images at predefined breathing phases. Commercial 4DCT techniques employ either ciné or low-pitch helical acquisition, with image reconstruction based on phase binning[1,3–5] or amplitude binning[2,6–8] methods. In the literature, amplitude binning approaches have been shown to be superior in reducing image artifacts than phase binning methods,[8–12] but are susceptible to insufficient image data at some couch positions if respiratory cycle was missing desired amplitude due to irregular breathing. In spite of these issues, both amplitude and phase-based 4DCT protocols are still employed in the commercially available 4DCT software.

Conventional 4DCT protocols are sensitive to irregular breathing. Breathing patterns depend on the mental and physiological condition of the subject during the scanning session, and large variability is often observed. 4DCT image acquisition by low-pitch helical CT protocol can lead to motion underestimation due to, e.g., breath pauses or overestimation if the subject takes abrupt deep breaths while the tumor is being

scanned. The image binning process can lead to streaking arti- facts, missing image slices, and distorted shapes and volume measurements.[9,13] The limitations of 4DCT pertaining to tu- mor volume definition have been investigated using internal or external breathing surrogates, where significant deviation of ciné-mode 4DCT (>50%) from realistic tumor motion was reported.[14–16]

Various techniques have been proposed for retrospective sorting-based approaches with the aim of reducing irregular breathing artifacts in 4DCT images.[17–21] In particular, Thomas *et al.* demonstrated the acquisition of sorting-artifact-free CT images at arbitrary user-selected breathing phases based on a lung motion model[21] first published by Low *et al.*[22] This approach is termed 5DCT (three spatial dimensions along with the breathing amplitude and breathing rate). The 5DCT image acquisition aims at capturing the extent of lung tissue motion by performing multiple high-pitch (1.2) helical scans with a simultaneously recorded surrogate signal. The tissue specific displacement is obtained through deformable image registration and correlated with the measured surrogate signal such that lung tissue positions can be computed at any given breathing signal. The accuracy of the 5DCT technique has been found to be on the order of 2 mm.
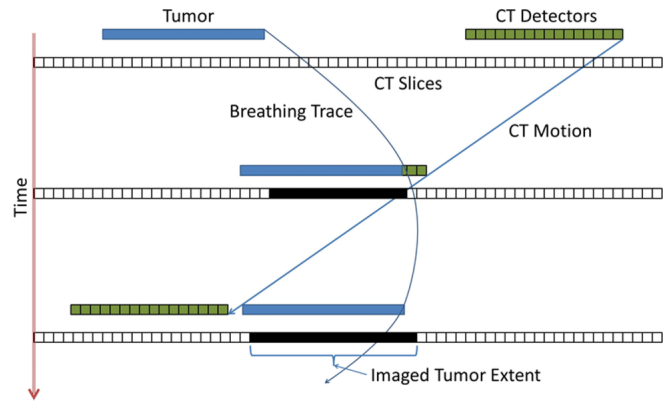


FIG. 1. Schematic of 4DCT simulation model. The CT detectors move from right to left while the tumor moves along its path a distance proportional to the breathing amplitude. The CT slices are set to 0 until the tumor overlaps the moving CT detectors. For each time point, corresponding to the motion of the CT by one CT slice, the overlap is assessed and overlapping slices are set to 1. When the simulation is completed, the total of the tumor size and breathing induced motion is the extent of the imaged tumor. This process is repeated starting at sequential time points 0.1 s apart to build the statistical evaluation of the imaged tumor extent as a function of patient, tumor size, and nominal tumor motion extent.
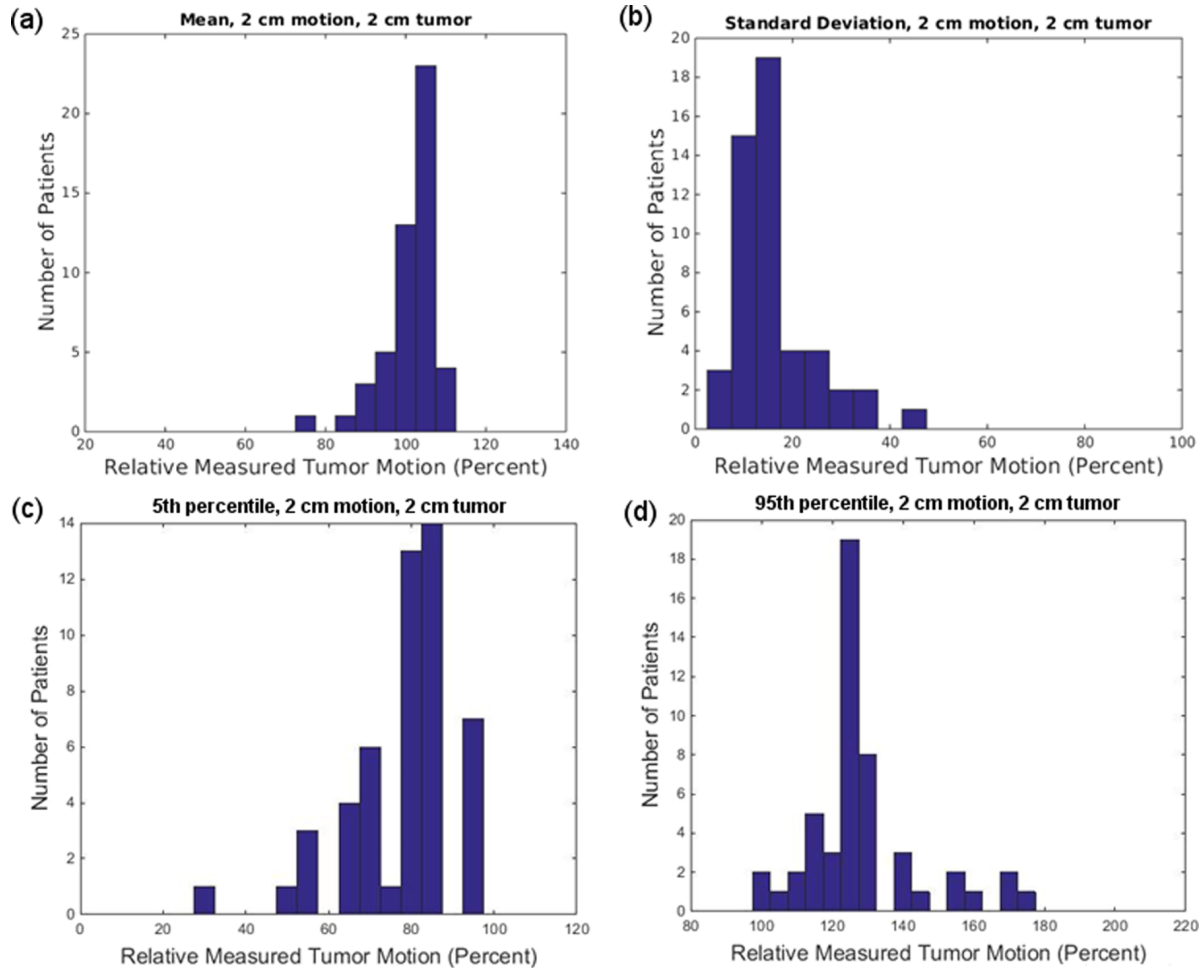


FIG. 2. (a) Mean relative breathing amplitude ratio, (b) standard deviation of relative breathing amplitude ratio, (c) mean relative breathing amplitude ratio for measured motion less than the 5th percentile, and (d) mean relative breathing amplitude ratio for measured motion greater than the 95th percentile. These examples are simulated for the 2 cm tumor and 2 cm nominal tumor motion magnitude $f$ with a pitch value of 0.06.

In this paper, we investigate the variability of tumor motion measurements by low-pitch helical 4DCT, in which the CT scanner is run at pitches of approximately 0.06 and 0.1, selected to reflect commercial systems, such that it continuously images the mobile anatomy. A simulation was developed to determine the protocol-measured tumor motion employing actual breathing traces from 50 patients. The simulated tumor motion was compared against a percentile-based motion magnitude. Such an approach is consistent with the 5DCT technique, where the motion is characterized as a function of breathing amplitude and breathing rate. The differences between the simulated and percentile motion were used to characterize motion measurement errors due to irregular breathing.

## 2. METHODS AND MATERIALS

A group of 50 patients was recruited in an IRB-approved clinical study; 26 with lung cancers and 24 with abdominal cancers. Research 5DCT scans were conducted with the patient free breathing. For this work, only the breathing traces were employed. The patient's breathing trace amplitudes were measured using a pneumatic belt (bellows). The bellows was wrapped around the patient's abdomen and as the patient inhaled and exhaled, the bellows was stretched and relaxed, causing the air pressure in the bellows to decrease and increase,

respectively. A pressure transducer measured the internal air pressure and this was recorded as the breathing surrogate. This signal had been previously shown to be linearly related to the tidal volume.[23] The breathing traces were at least 5 min long, sampled at 100 Hz, and included normal breathing irregularities. The breathing traces had been previously corrected for baseline drift and converted to tidal volume.

A simulation was performed to determine the measured tumor motion amplitude based on the breathing trace as though the patient had been scanned using a commercial low-pitch helical protocol. For the 4DCT simulation, the scanner parameters were taken from the 16-slice Philips Big Bore 4DCT protocol: pitch of 0.06, rotation time of 0.5 s, and detector width of 2.4 cm and the Siemens Somatom Sensation Open that employed the same rotation time and detector width but a pitch of 0.1. This translated to irradiation times of approximately 8.3 and 0.5 s for stationary tissues using the 0.06 and 0.1 pitches, respectively. The images were assumed to be reconstructed using 1.5 mm thick slices.

The 4DCT approach was simulated by subdividing the craniocaudal imaging space into 1.5 mm thick slices (Fig. 1). The scanner was first positioned at one end of the imaging space and its position identified at subsequent times according to its velocity and time. The tumor was positioned sufficiently away from the end of the imaging space so that the tumor
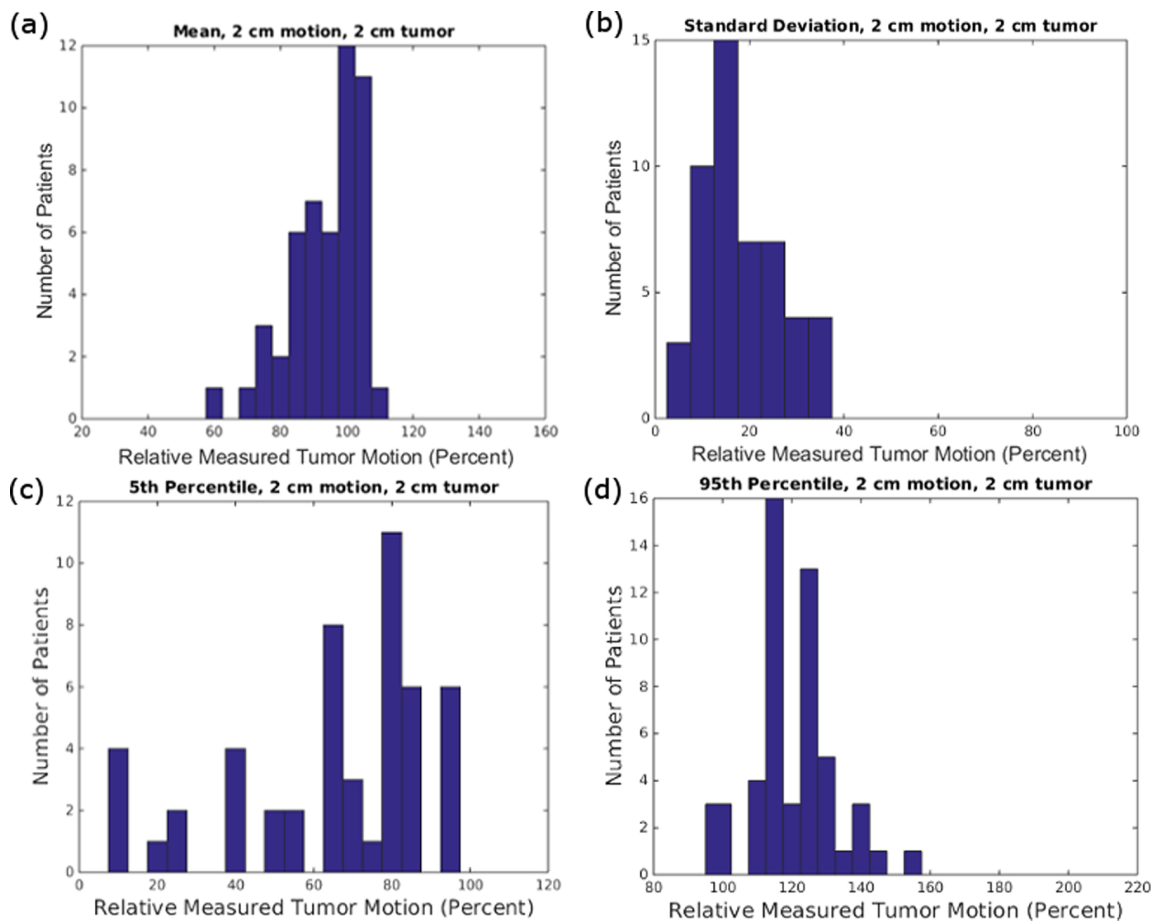


FIG. 3. (a) Mean relative breathing amplitude ratio, (b) standard deviation of relative breathing amplitude ratio, (c) mean relative breathing amplitude ratio for measured motion less than the 5th percentile, and (d) mean relative breathing amplitude ratio for measured motion greater than the 95th percentile. These examples are simulated for the 2 cm tumor and 2 cm nominal tumor motion magnitude using a pitch of 0.1.

TABLE I(a). Mean 5th percentile amplitude of the lowest 30% relative to tumor motion in percentage for a pitch of 0.06.

| Size(cm)\motion(cm) | 1 | 2 | 3 | 4 |
|---|---|---|---|---|
| 1 | 70.94 | 62.56 | 61.64 | 61.77 |
| 2 | 68.06 | 62.36 | 62.32 | 61.88 |
| 3 | 66.86 | 64.16 | 61.61 | 61.84 |
| 4 | 70.58 | 62.72 | 62.52 | 61.13 |

TABLE I(c). Mean 95th percentile amplitude of the upper 30% relative to tumor motion in percentage for a pitch of 0.06.

| Size(cm)\motion(cm) | 1 | 2 | 3 | 4 |
|---|---|---|---|---|
| 1 | 151.70 | 147.68 | 146.51 | 147.26 |
| 2 | 154.47 | 147.35 | 146.76 | 147.63 |
| 3 | 174.07 | 147.92 | 147.19 | 147.18 |
| 4 | 154.24 | 148.03 | 146.43 | 145.95 |

was always in the field of view. Its position was determined by converting the breathing amplitude waveform to a tumor location. The image space slices corresponding to the tumor size and position were identified and if they overlapped the CT scanner position, those slices were identified as having imaged the tumor.

The time sequence of the simulation was started at a selected point in the breathing cycle. Each subsequent simulation was repeated with the subsequent time bin in the breathing cycle. The breathing waveform was in the form of the digitized bellows air pressure and this needed to be converted to the craniocaudal motion of the tumor. To accomplish this conversion, we made two assumptions. First, we assumed that the tumor motion in this dimension was linearly proportional to the breathing amplitude. This motion linearity assumption has been previously tested and reported in the literature.[22,24,25] Further, the 90th percentile (95th minus the 5th) of the breathing amplitude waveform was employed as the definition of the nominal breathing depth. Our percentile-based approach of inhalation/exhalation definition explicitly accounted for the relative frequencies these tidal breathing amplitudes occurred and had the additional advantage that breathing statistics were less susceptible to the influences of the few extreme shallow or deep breaths.[8,26] The breathing waveform was converted to tumor motion by multiplying the waveform by the ratio of the nominal tumor motion (e.g., 1 cm) to the 90th percentile waveform amplitude. This provided a tumor motion distribution such that the 90th percentile of motion was equal to the nominal tumor motion.

The tumor was moved along the imaging space according to the scaled breathing amplitude. Overlap between the tumor and the CT slices was identified as having imaged the tumor in that location and registered in a binary fashion. The effect of partial overlap was expected to be small and average out over the repeated simulations and did not affect the resulting estimated tumor motion variation. The time sequence was moved forward until the CT scanner had well passed the tumor positions. The combined overlap envelope was assumed to be an amplitude-sorted measure of the total of the tumor motion

and size, so the tumor size was subtracted from the total envelope to extract the measured tumor motion. To study the clinically commonly observable tumor dimension and motion range, the process was repeated for different combinations of nominal tumor motions of 1–4 cm in 1 cm increments and for tumor sizes of 1–4 cm in 1 cm increments.

For each patient, there was a distribution of measured motion errors for each tumor size and motion magnitude. Since the typically one-time tumor motion measurement of any 4DCT would be employed to develop a motion strategy, we treated the measured motion errors as systematic errors. Therefore, we elected to examine the greatest over- and underestimations of tumor motion by selecting the 5% of outlying cases for each of over- and underestimations. The selection of the outlier distribution was intended to reflect the scenarios where the treatment planning performed under such conditions (i.e., with a total of a 10% chance of occurring) would be conducted with an erroneous motion measurement without feedback to the clinic that this had occurred. This simulation was implemented and analyzed using MATLAB software (Math-Works, Natwick, MA).

## 3. RESULTS

Figure 2 shows histograms of the mean of the estimated tumor motion errors and the associated standard deviation as well as the means of the 5% over- and 5% underestimated motion errors for each of the 50 patients for the 2 cm tumor size and 2 cm tumor motion simulation performed using the pitch of 0.06. The value of 100% corresponds to the 90th percentile breathing amplitude, consistent with the 5DCT approach. The simulated motion estimation is compared to the 5DCT motion measurement and the estimation error is expressed as percent deviation from the 5DCT approach. Similar results were observed for the other tumor motion magnitudes and tumor sizes.

Many of the 50 patients breathed quite regularly, so their relative motion measurements were close to 100%. This is observed both in the distribution of the mean tumor motion

TABLE I(b). Mean 5th percentile amplitude of the lowest 30% relative to tumor motion in percentage for a pitch of 0.1.

| Size(cm)\motion(cm) | 1 | 2 | 3 | 4 |
|---|---|---|---|---|
| 1 | 44.98 | 37.46 | 38.48 | 41.47 |
| 2 | 37.06 | 33.26 | 37.76 | 42.89 |
| 3 | 33.98 | 34.30 | 39.67 | 42.30 |
| 4 | 38.11 | 35.53 | 38.88 | 41.03 |

TABLE I(d). Mean 95th percentile amplitude of the upper 30% relative to tumor motion in percentage for a pitch of 0.1.

| Size(cm)\motion(cm) | 1 | 2 | 3 | 4 |
|---|---|---|---|---|
| 1 | 140.50 | 132.75 | 133.13 | 134.89 |
| 2 | 138.76 | 133.84 | 134.45 | 136.01 |
| 3 | 140.64 | 134.38 | 135.71 | 137.31 |
| 4 | 145.07 | 136.38 | 136.41 | 137.50 |

estimation [Fig. 2(a)] and their small uncertainty values [Fig. 2(b)] as well as in the outlier distributions [Figs. 2(c) and 2(d)]. On the other hand, the maximum and minimum 5% motion error ratio distributions showed that 30% of the patients would have had breathing amplitude underestimation of at least 36% while 30% would have had overestimations of over 47%. The 16 trials (4 tumor sizes and 4 tumor motion magnitudes) provided essentially identical results due to the fact that the tumor size was subtracted from the overall motion envelope and the motion error was evaluated as the ratio of the subsequent motion to the nominal motion magnitude.

Figure 3 showed the example breathing motion estimation simulated using a pitch of 0.1. Compared with the results using the pitch of 0.06, overestimation of the imaged tumor motion decreased. On the other hand, the distribution of underestimated tumor motion showed more deviation from the true motion amplitude. Tables I(a) and I(b) show the mean 5th tumor motion amplitude of the bottom 30% of the patients by the simulated tumor size and tumor motion for the 0.06 and 0.1 pitch values, respectively. Similarly, Tables I(c) and I(d) show the mean 95th tumor motion amplitude of the top 30% of the examined patients.

## 4. DISCUSSION AND CONCLUSIONS

Respiratory-gated 4DCT is an indispensable tool for characterizing breathing motion for the thorax and upper abdomen. The breathing pattern of diseased patients is often irregular. Commercial 4DCT techniques are susceptible to irregular breathing patterns, which lead to errors in treatment planning and delivery. Since 4DCT is typically performed once per patient, any resulting error can cause systematic treatment planning errors. This work simulated the performance of low-pitch helical 4DCT acquisition in a group of 50 patients. In the examined 50-patient motion error distributions, the mean values of the fringe subdistributions of the largest and smallest 5% of the relative motion errors were computed. For the examined patient cohort, in the worst-case scenario, the breathing amplitude was underestimated by as much as 74% and overestimated by 177%. Our analysis using two different scanning pitch parameters showed stronger underestimation across all combinations of simulated tumor size and motion when scanned at a higher pitch of 0.1 compared to 0.06, while the opposite was true for overestimations. Explicit management of irregular breathing such as is done with the 5DCT protocol has the potential for reducing the uncertainty of the relationship between the imaged and actual tumor motions.

The present study investigated the 4DCT tumor motion measurement variability using a surrogate signal. The 1D analysis in the superior–inferior direction was motivated by the nearly linear relationship between the breathing amplitude and the lung tissue displacement, which has been established in the literature.[22,27,28] Given that lung tissue motion tended to be largest in the superior–inferior dimension, the results were likely to be similar to the analysis of the 3D motion. Our simulation technique provided the advantage that many 4DCT sessions could be simulated, as opposed to image-based assessments where 4DCT data are typically a single set or

a limited few. The statistics obtained from our simulations provided insight to the variability of measured tumor motion using commercial helically based 4DCT techniques.

The technique did not consider motion hysteresis, which affects some tumors. Breathing irregularities for these tumors would be more challenging to model. The technique also used only single breathing traces for each patient, so intrapatient variability over multiple sessions was not evaluated.

Selection of the 95th and 5th percentile breathing surrogate amplitudes to normalize the motion was arbitrary. There are no accepted definitions of inhalation and exhalation based on percentiles, but given that the results were nearly independent of tumor motion magnitude, selection of other percentiles to define the relationship between breathing magnitude and tumor motion would have provided similar results. The choice of evaluating the outlying five percent error distributions only served to show the magnitude of error in 4DCT motion estimation. Smaller outlying distributions can exhibit even larger errors, while a choice of greater percentiles would show smaller errors. We conclude that commercial clinical 4DCT images should be used with caution for patients with highly irregular breathing patterns.

[a)]Author to whom correspondence should be addressed. Electronic mail: tdou@mednet.ucla.edu

[1]E. C. Ford, G. S. Mageras, E. Yorke, and C. C. Ling, "Respiration-correlated spiral CT: A method of measuring respiratory-induced anatomic motion for radiation treatment planning," Med. Phys. **30**, 88–97 (2003).

[2]D. A. Low, M. Nystrom, E. Kalinin, P. Parikh, J. F. Dempsey, J. D. Bradley, S. Mutic, S. H. Wahab, T. Islam, G. Christensen, D. G. Politte, and B. R. Whiting, "A method for the reconstruction of four-dimensional synchronized CT scans acquired during free breathing," Med. Phys. **30**, 1254–1263 (2003).

[3]S. S. Vedam, P. J. Keall, V. R. Kini, H. Mostafavi, H. P. Shukla, and R. Mohan, "Acquiring a four-dimensional computed tomography dataset using an external respiratory signal," Phys. Med. Biol. **48**, 45–62 (2003).

[4]P. J. Keall, G. Starkschall, H. Shukla, K. M. Forster, V. Ortiz, C. W. Stevens, S. S. Vedam, R. George, T. Guerrero, and R. Mohan, "Acquiring 4D thoracic CT scans using a multislice helical method," Phys. Med. Biol. **49**, 2053–2067 (2004).

[5]T. Pan, T. Y. Lee, E. Rietzel, and G. T. Y. Chen, "4D-CT imaging of a volume influenced by respiratory motion on multi-slice CT," Med. Phys. **31**, 333–340 (2004).

[6]W. Lu, D. A. Low, P. J. Parikh, M. M. Nystrom, I. M. El Naqa, S. H. Wahab, M. Handoko, D. Fooshee, and J. D. Bradley, "Comparison of spirometry and abdominal height as four-dimensional computed tomography metrics in lung," Med. Phys. **32**, 2351–2357 (2005).

[7]W. Lu, P. J. Parikh, I. M. El Naqa, M. M. Nystrom, J. P. Hubenschmidt, S. H. Wahab, S. Mutic, A. K. Singh, G. E. Christensen, J. D. Bradley, and D. A. Low, "Quantitation of the reconstruction quality of a four-dimensional computed tomography process for lung cancer patients," Med. Phys. **32**, 890–901 (2005).

[8]W. Lu, P. J. Parikh, J. P. Hubenschmidt, J. D. Bradley, and D. A. Low, "A comparison between amplitude sorting and phase-angle sorting using external respiratory measurement for 4D CT," Med. Phys. **33**, 2964–2974 (2006).

[9]M. Guckenberger, M. Weininger, J. Wilbert, A. Richter, K. Baier, T. Krieger, B. Polat, and M. Flentje, "Influence of retrospective sorting on image quality in respiratory correlated computed tomography," Radiother. Oncol. **85**, 223–231 (2007).

[10]A. F. Abdelnour, S. A. Nehmeh, T. Pan, J. L. Humm, P. Vernon, H. Schoder, K. E. Rosenzweig, G. S. Mageras, E. Yorke, S. M. Larson, and Y. E. Erdi,

"Phase and amplitude binning for 4D-CT imaging," Phys. Med. Biol. **52**, 3515–3529 (2007).

[11] M. J. Fitzpatrick, G. Starkschall, J. A. Antolak, J. Fu, H. Shukla, P. J. Keall, P. Klahr, and R. Mohan, "Displacement-based binning of time-dependent computed tomography image data sets," Med. Phys. **33**, 235–246 (2006).

[12] E. Rietzel, T. S. Pan, and G. T. Y. Chen, "Four-dimensional computed tomography: Image formation and clinical protocol," Med. Phys. **32**, 874–889 (2005).

[13] T. Yamamoto, U. Langner, B. W. Loo, Jr., J. Shen, and P. J. Keall, "Retrospective analysis of artifacts in four-dimensional CT images of 50 abdominal and thoracic radiotherapy patients," Int. J. Radiat. Oncol., Biol., Phys. **72**, 1250–1258 (2008).

[14] J. Cai, R. McLawhorn, P. W. Read, J. M. Larner, F.-f. Yin, S. H. Benedict, and K. Sheng, "Effects of breathing variation on gating window internal target volume in respiratory gated radiation therapy," Med. Phys. **37**, 3927–3934 (2010).

[15] J. Sarker, A. Chu, K. Mui, J. A. Wolfgang, A. E. Hirsch, G. T. Y. Chen, and G. C. Sharp, "Variations in tumor size and position due to irregular breathing in 4D-CT: A simulation study," Med. Phys. **37**, 1254–1260 (2010).

[16] S. St. James, P. Mishra, F. Hacker, R. I. Berbeco, and J. H. Lewis, "Quantifying ITV instabilities arising from 4DCT: A simulation study using patient data," Phys. Med. Biol. **57**, L1–L7 (2012).

[17] J. Ehrhardt, R. Werner, D. Saring, T. Frenzel, W. Lu, D. Low, and H. Handels, "An optical flow based method for improved reconstruction of 4D CT data sets acquired during free breathing," Med. Phys. **34**, 711–721 (2007).

[18] A. Hertanto, Q. H. Zhang, Y. C. Hu, O. Dzyubak, A. Rimner, and G. S. Mageras, "Reduction of irregular breathing artifacts in respiration-correlated CT images using a respiratory motion model," Med. Phys. **39**, 3070–3079 (2012).

[19] U. W. Langner and P. J. Keall, "Accuracy in the localization of thoracic and abdominal tumors using respiratory displacement, velocity, and phase," Med. Phys. **36**, 386–393 (2009).

[20] J. R. McClelland, J. M. Blackall, S. Tarte, A. C. Chandler, S. Hughes, S. Ahmad, D. B. Landau, and D. J. Hawkes, "A continuous 4D motion model from multiple respiratory cycles for use in lung radiotherapy," Med. Phys. **33**, 3348–3358 (2006).

[21] D. Thomas, J. Lamb, B. White, S. Jani, S. Gaudio, P. Lee, D. Ruan, M. McNitt-Gray, and D. Low, "A novel fast helical 4D-CT acquisition technique to generate low-noise sorting artifact-free images at user-selected breathing phases," Int. J. Radiat. Oncol., Biol., Phys. **89**, 191–198 (2014).

[22] D. A. Low, P. J. Parikh, W. Lu, J. F. Dempsey, S. H. Wahab, J. P. Hubenschmidt, M. M. Nystrom, M. Handoko, and J. D. Bradley, "Novel breathing motion model for radiotherapy," Int. J. Radiat. Oncol., Biol., Phys. **63**, 921–929 (2005).

[23] R. Werner, B. White, H. Handels, W. Lu, and D. A. Low, "Technical note: Development of a tidal volume surrogate that replaces spirometry for physiological breathing monitoring in 4D CT," Med. Phys. **37**, 615–619 (2010).

[24] V. Boldea, G. C. Sharp, S. B. Jiang, and D. Sarrut, "4D-CT lung motion estimation with deformable registration: Quantification of motion nonlinearity and hysteresis," Med. Phys. **35**, 1008–1018 (2008).

[25] Y. Seppenwoolde, H. Shirato, K. Kitamura, S. Shimizu, M. van Herk, J. V. Lebesque, and K. Miyasaka, "Precise and real-time measurement of 3D tumor motion in lung due to breathing and heartbeat, measured during radiotherapy," Int. J. Radiat. Oncol., Biol., Phys. **53**, 822–834 (2002).

[26] T. Y. Zhao, W. Lu, D. S. Yang, S. Mutic, C. E. Noel, P. J. Parikh, J. D. Bradley, and D. A. Low, "Characterization of free breathing patterns with 5D lung motion model," Med. Phys. **36**, 5183–5189 (2009).

[27] D. Sarrut, V. Boldea, S. Miguet, and C. Ginestet, "Simulation of four-dimensional CT images from deformable registration between inhale and exhale breath-hold CT scans," Med. Phys. **33**, 605–617 (2006).

[28] E. Schreibmann, G. T. Y. Chen, and L. Xing, "Image interpolation in 4D CT using a BSpline deformable registration model," Int. J. Radiat. Oncol., Biol., Phys. **64**, 1537–1550 (2006).